Design of Detection-Jamming Shared Waveform Based on Virtual Force Field Algorithm

XIONG GuoMiao*, LI Yunpeng, CHEN Chao

Chinese People's Liberation Army, Aviation University of Air Force, Jilin 130000, China

* Correspondence: 1063618799@qq.com

Abstract: Due to the technical barriers between radars and jammers and the poor performance of the traditional detection-jamming shared signal in integrated radar-electronic warfare systems, a new detection-jamming shared signal waveform based on the virtual force field algorithm (VFFA) is proposed in this paper. First, a multi-objective and multi-dimensional characteristic parameter optimization model, based on a virtual force field, is established, and then the design principle of the shared signal is presented in detail. The simulation results show that the detection-jamming shared signal based on the VFFA presents the deceptive jamming of multiple false targets in non-collaborative radar. Further, there is better detection performance with the advantages of multiple pulse repetition frequency (PRF) and pulse accumulation number, which are highly sensitive to the multi-jagged PRF signals emitted by the non-collaborative radar. According to the VFFA described in this paper, the optimum detection-jamming shared signal waveform can be output in real time for specific free space targets, to improve the efficiency of integrated radar and electronic warfare systems.

Keywords: Virtual force field algorithm; detection and jamming integration; shared signal; waveform design; deceptive jamming.

0 Introduction

At present, to eliminate the bottlenecks in radar and jammer operations within their respective systems, the integration of radar and electronic warfare is changing the concept of depth integration from traditional "hardware sharing" to "power sharing". This integration focuses on realizing "signal sharing", which is a sharing signal waveform that integrates the function of detection and jamming, also known as a "shared signal" [1–3]. The key to further integration of radar and electronic warfare is the design of a detection-jamming shared signal. With the rapid development of antenna array technology, data fusion technology, and power control technology, advancements in new "detection-jamming sharing" signal styles and the realization of "power sharing" have become not only possible but extremely crucial and key research directions, and various experts and scholars have conducted related theoretical research.

Currently, theoretical research regarding detection-jamming shared signals is limited to study of the integration between detection and oppressive jamming [4–13]. Only when the bandwidth is suppressed completely and a high duty ratio jamming signal is used can the suppression interference to the target be realized and the best interference effect be achieved. The traditional detection-jamming shared signal cannot realize active jamming when detecting or performing reconnaissance, which is one of the main disadvantages of the traditional detection-jamming shared signal due to the conflict of time sequence between the detection and jamming. However, it is the conflict of time sequence that greatly reduces the effectiveness of target jamming.

Therefore, in order to improve the jamming effect of the detection-jamming shared signal and establish a detection advantage by making full use of the false target echo signal and carry on the signal reconstruction and signal accumulation, the shared signal waveform of detection and deceptive jamming is proposed in this paper, which takes the non-collaborative detection signal as the sample

jamming signal. Further, its waveform characteristics is similar to the non-collaborative pulse. Simultaneously, in order to solve the time-domain conflict between detection-jamming shared signals, its echo signals, and reconnaissance signals, the multi-dimensional parameter characteristics of the false target of the detection-jamming shared signals are optimized by introducing and taking full use of the advantages of the virtual force field algorithm (VFFA), such as simple operation, fast convergence speed, and real-time obstacle avoidance [14–21]. Finally, the detection-jamming shared signal is designed based on VFFA, general reconnaissance, jamming, and detection to achieve effective separation in the time sequence, and it is shown to present a good deceptive effect on the non-collaborative radar receiver. After the related signal processing of the integrated detection-jamming system, the echo signal can achieve excellent non-ambiguous distance and velocity measurements and has a good effect of pulse accumulation, showing good detection performance. Lastly, the detection-jamming shared signal based on VFFA can effectively detect and jam the non-collaborative radar.

1 Problem Description

Since the last century, radar and electronic warfare integration research has initiated in many technologically advanced countries. There are three stages of development for the integration of radar and electronic warfare: “hardware sharing” to “software sharing for avionics systems” to “energy sharing”. With the continuous progress of science and technology, efforts to solve hardware sharing and data fast-processing have been developed [22–31]. At present, the timing conflict among reconnaissance, detection, and jamming is an insurmountable obstacle to realize signal energy sharing.

As shown in Fig. 1, in order to ensure the time sequence separation of detection and the interference, when it is known that the non-collaborative target is R km away from the operator, then the echo signal position of the detection interference shared signal can be calculated, as its relative time delay is $T_{delay} = R / C$. Additionally, we can assume that the non-collaborative target transmits an N-jagged PRF signal, $\mathrm{PRI} = \sum_{i=1}^{n} \mathrm{PRI}_i$. After the relative time delay, we receive the non-collaborative detection signal and transmit the detection-jamming shared signal to generate a certain number of false targets, which enter the non-collaborative radar receiver together with the real echo signal. At the same time, we receive the echo signal of our detection-jamming shared signal, as shown in Fig. 1(e). By comparing Fig. 1(c) with Fig. 1(e), there are many overlapping problems in several time sequences:

(1) Timing conflict: Receiving the integrated echo signal and the non-collaborative detection signal is contradictory to the transmitting pulse and receiving echo pulse, causing the timing sequence of radar transmission and receipt to be in conflict.

(2) Pulse overlap: The integrated echo signal and the non-collaborative detection signal overlap when the integrated echo signal and the non-collaborative detection signal arrived at the same time.

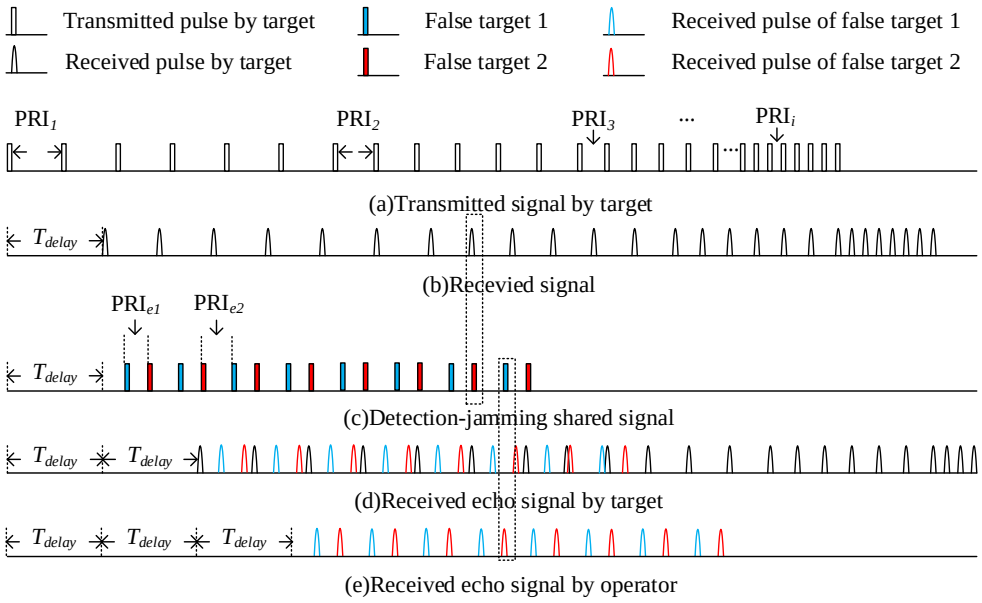

Fig. 1. Analysis diagram of time sequence between detection and jamming of N-jagged PRF radar signal.

2 Principles of the Analysis of VFFA

By introducing and applying the VFFA to the design of the detection-jamming shared signal, the obstacles in the timing sequence of receiving and transmitting can be effectively avoided, and the problems of timing conflict and pulse overlap can be effectively solved.

The basic idea of VFFA [32–37] is to treat the false target set in space as a node and also as a particle, which can be regarded as a virtual point charge in space. The repulsive forces from other virtual charges will act between nodes. Therefore, nodes will be mutually exclusive and separated from each other, achieving the effect of obstacle avoidance. There is no position conflict between nodes, so the positions of false targets are separated in space.

As shown in Fig. 2, the original point position of the spatial coordinate system is the real target position. Within this airspace scope, a certain number of false targets are arranged in the airspace, and each false target has the deceptive effect of relative distance, velocity, and angle. In the VFFA, a triplet, $< P_i, L, F_i >$, is introduced to represent the position, force magnitude, and the direction of the i^{th} node, where $P_i = (x_i, y_i, z_i)$ is the spatial rectangular coordinate of the i^{th} node. Additionally, L is the maximum inductive range of repulsive forces between nodes, that is, when the spatial distance between nodes exceeds this range, there is no mutual repulsive relationship between the two nodes; and $F_i = (F_{xi}, F_{yi}, F_{zi})$ is the projection component in the X axis, Y axis, and Z axis directions, respectively.

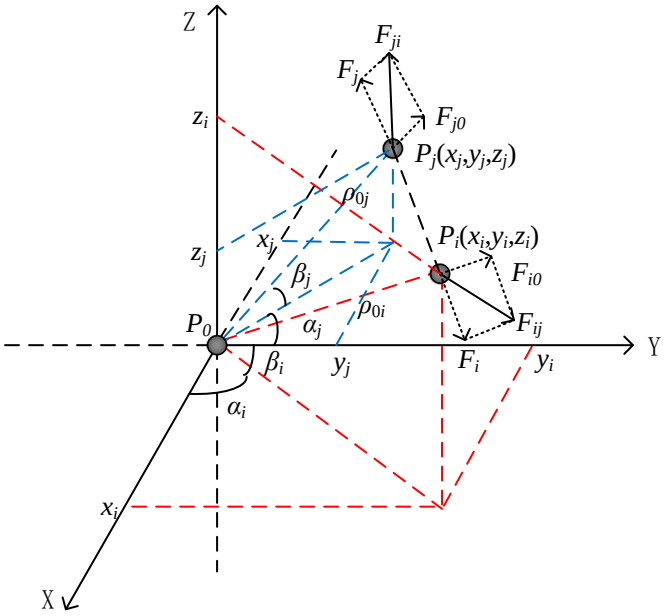

Fig. 2. Interaction force between nodes in the virtual force field.

According to the transformation relationship between the Cartesian coordinate system and the polar coordinate system, it can be deduced that the spatial polar coordinates corresponding to the node $P_i(x_i, y_i, z_i)$ are $Q_i(\alpha_i, \beta_i, \rho_{0i})$, as follows:

$$\begin{cases} F_{xi} = \rho_{0i} \cos\beta_i \cos\alpha_i \\ F_{yi} = \rho_{0i} \cos\beta_i \sin\alpha_i \\ F_{zi} = \rho_{0i} \sin\beta_i \end{cases} \tag{1}$$

Therefore, the spatial distance D_{ij} between P_i and P_j can be expressed as:

$$\begin{aligned} D_{ij} &= \left\| P_i - P_j \right\|_2 \\ &= \sqrt{(x_i - x_j)^2 + (y_i - y_j)^2 + (z_i - z_j)^2} \end{aligned} \tag{2}$$

where $\|\bullet\|_2$ is a 2-norm, also known as a Euclidean norm. We assume the repulsion model $\overrightarrow{F_{ij}}$ from node P_j to node P_i is as shown in Equation (3):

$$\overrightarrow{F_{ij}} = \begin{cases} (\frac{F_{cr}}{D_{ij}^2}, \theta_{ij}(\alpha_{ij}, \beta_{ij})), & if \quad P_j \in \psi_i \\ \vec{0}, & otherwise \end{cases} \tag{3}$$

In Equation (3), F_{cr} is the repulsion coefficient (F_{cr}=1); $\theta_{ij}(\alpha_{ij}, \beta_{ij})$ denote the relative azimuth and pitch angles, respectively, in space between P_i and P_j; and ψ_i denotes the neighbor nodes

surrounding the node P_i within the range *L*. According to Equation (2), Equation (3) can be converted into:

$$\overrightarrow{F_{ij}} = \begin{cases} \left\| \dfrac{F_{cr}}{(P_i - P_j)^2} \right\|_2, & if \quad P_j \in \psi_i \\ \vec{0}, & otherwise \end{cases} \tag{4}$$

Therefore, the resultant force received by a node P_i is the vector sum of the repulsive forces of *k* nodes within the maximum induction range of *L* at this spatial position. The resultant force model $\overrightarrow{F_i}$ is expressed as follows:

$$\overrightarrow{F_i} = \begin{cases} \sum_{j=1, j\neq i}^{k} \overrightarrow{F_{ij}}, & k \geq 1 \\ \vec{0}, & k = 0 \end{cases} \tag{5}$$

In the design of the false target space position model for detecting interference shared signals, the nodes are affected by the resultant force $\overrightarrow{F_i}$ and seek the best position in space motion to avoid obstacles. When all nodes reach equilibrium, the motion of the false target node stops, and the position is confirmed.

3. Analysis of Shared Signal Design Principle

A simple flowchart for the design of the detection-jamming shared signal waveform based on VFFA is shown in Fig. 3. Among the processes shown in Fig. 3, the environment rasterization module realizes the functions of quantification, digitization, and visualization of the virtual space environment. The target parameter optimization module uses the VFFA to update and iterate the false target parameters to realize the optimization design of multiple false target parameters. The data output module can save the data of the optimized results and transmit the detection-jamming shared signal waveform under the optimal state. The verification module can verify the false target parameters in real time according to the non-collaborative dynamic, improve the high fidelity of the false target parameters, and ensure the deceptive effect.

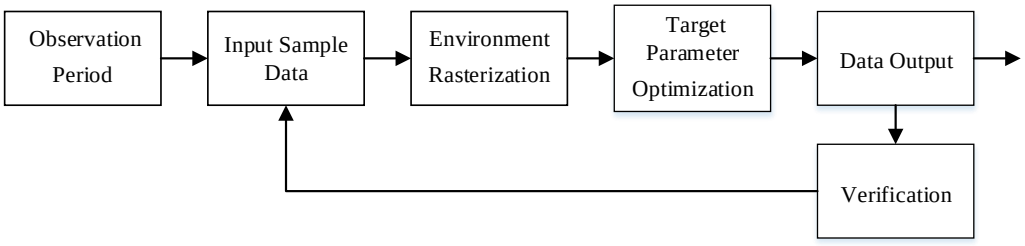

Fig. 3. Basic flow diagram of VFFA.

3.1 Rasterization of the virtual environment

Based on VFFA, the maximum space range of the environment is set as S_{max}, which depends on

the PRF of the non-collaborative detection signal. The width of a single grid is *r*, which depends on the detection signal pulse width, because the integrated radar-electronic warfare system can only generate a pulse signal within each sequence, which can only produce a false target. Therefore, the grid scale in the virtual environment is a flat body with width *r*, so the grid number is S_{max}/r. *G* is composed of a grid g_i, $G=\{g_i|g_i=0 \text{ or } 1\}$, where $g_i = 0$ indicates that the grid is a free area, and $g_i = 1$ indicates that the grid is an obstacle area.

Therefore, when we know that the non-collaborative target is R km away from the operator, the position of the echo signal of the detection-jamming shared signal can be calculated, and the moving distance corresponding to the relative time delay is given by x_r. The shared signal transmitting pulse is bound to the echo pulse. When g_{x_i} (representing the grid position corresponding to the X wheelbase of node P_i) is equal to 1, $g_{x_i}+g_{x_r}$ gives 1 as well.

3.2 Optimization and verification of target parameters

After rasterizing the environment, the design process of the detection-jamming shared signal based on VFFA is shown in Fig. 4. The specific implementation steps are as follows:

Step 1: After prior knowledge collection and given the approximate position of the target from the integrated platform, when the integrated platform receives the non-collaborative radar pulse signal, it can judge the non-collaborative radar working mode, including the pulse parameters and intra-pulse characteristics. The position g_i where the non-collaborative detection signal appears should be set to the obstacle area and a value of one. Meanwhile, the range of the number of false targets, *m*, can be calculated as follows:

$$m<\left(\frac{\min(\mathrm{PRI}_i)-\tau}{(n+1)*\tau}\right), \quad \text{且} m>M \tag{6}$$

where τ is the non-collaborative detecting pulse width; and *n* is the number of the targets to detect and to search. Therefore, for every pulse that is transmitted, there are *n* echo pulses. Lastly, *M* is the multi-target searching ability of the non-collaborative radar and is also the channel number of signal processing. Equation (6) shows that the value of *m* is determined by the frequency and pulse width. When the non-collaborative signal PRF is higher, the value of *m* is lower. The wider the pulse width, the lower the value of *m*. Therefore, to achieve the best effect of deceptive jamming, the non-collaborative radar channel should be covered with false targets as much as possible under the condition of satisfying the major premise.

Step 2: By setting the stepping value Δx, the false target position $x_i = x_i + \Delta x$ should be moved within the range of the pulse repetition interval (PRI).

Step 3: The position of the i^{th} false target is confirmed as x_i, and the position of its echo signal is

bound to $X_{\mathrm{ri}} = x_i + x_r$. At the same time, both g_{x_i} and $g_{x_i} + g_{x_r}$ are set to one. The resultant force $\overrightarrow{F_i}$ of the i^{th} false target should be calculated in the virtual environment. Then, if x_i and X_{ri} are successful in obstacle avoidance, the algorithm goes to Step 4. If Step 3 is not met, then return to Step 2.

Step 4: Judging whether the two ending conditions are both satisfied.

Condition 1: If the current number of false targets has not been achieved by the chosen value of *m*, the algorithm goes to Step 2. On the contrary, if Condition 1 is not met, then this round of the false target parameter optimization should be ended. Each false target's exact location should be recorded. Meanwhile, the relative distance Δx_i between adjacent false targets on the X axis should be calculated. As such, the PRF_{ei} of the current integrated signal is obtained, as well as the maximum non-ambiguity distance R'_{max} and maximum non-ambiguity velocity V'_{max}, as shown in Equation (7):

$$V_{\max} = \frac{\lambda}{2} f_{r\max} \tag{7}$$

where $f_{r\max}$ is the maximum PRF value in the multi-PRF detection signal.

Condition 2: If R'_{max} and V'_{max} are greater than R_{max} and V_{max}, R_{max} and V_{max} should be updated, and the position information of the current false targets should be preserved. A new round of false target position optimization is started from Step 2. If Condition 2 is not met, then return to Step 5.

Step 5: When the stepping value Δx goes out of the range of PRI, the parameter information of the multiple false target positions is saved and updated under the current condition of R_{max} and V_{max}.

Step 6: The detection-jamming shared signal is transmitted under the mode of multiple false target parameter optimization to detect and jam the target.

Step 7: If the non-collaborative detection signal is lost in the reconnaissance channel, the algorithm enters the next observation period to intercept the non-collaborative detection signal sample and to measure its parameters again. If Step 7 is not met, then return to Step 6.

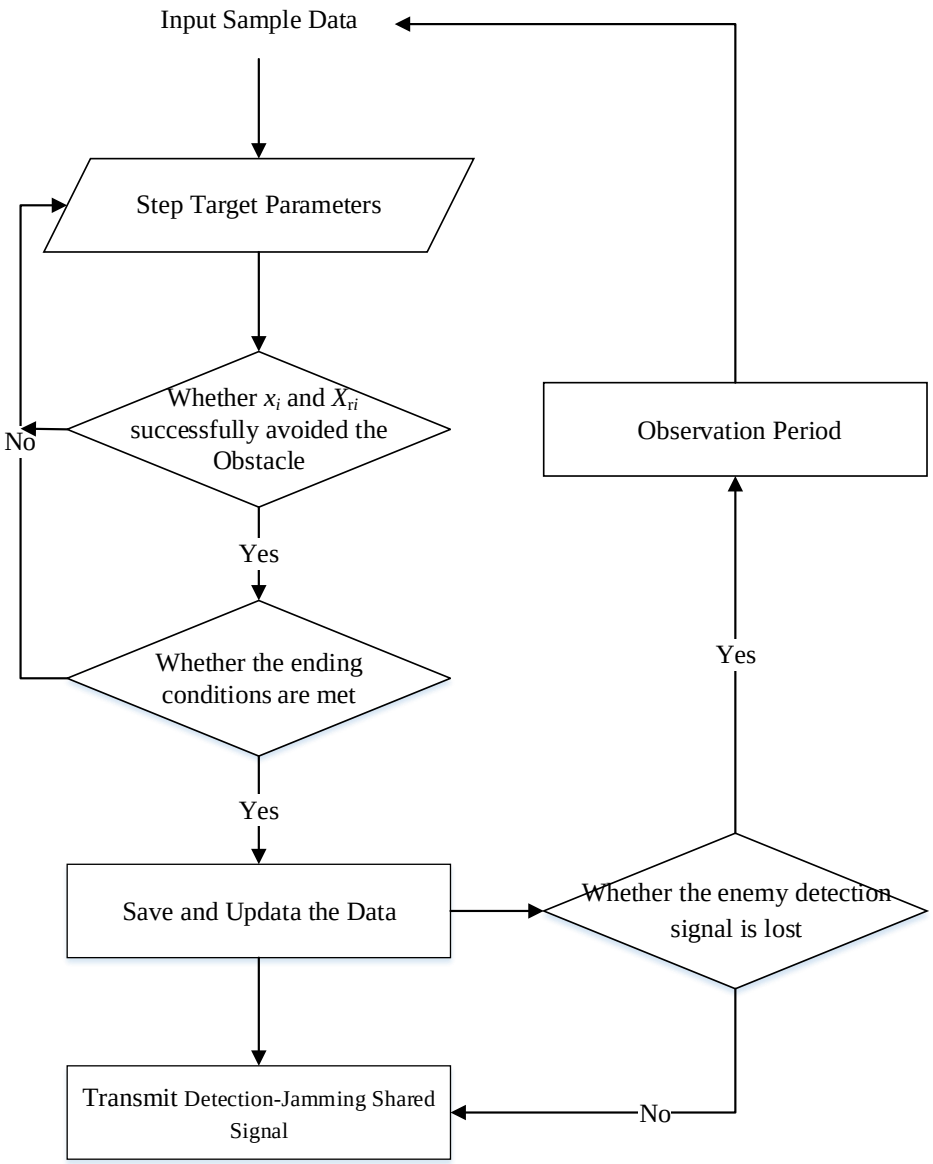

Fig. 4. Block diagram of shared signal design principle.

4 Experimental Simulation and Performance Analysis

Since the detection-jamming shared signal based on VFFA is based on the non-collaborative pulse signal and adopts duplicated and forwarded multi-false-target deceptive jamming, this experiment is built on the basis of effectively intercepting the non-collaborative radar signal and effectively measuring the pulse descriptive word (PDW) and in-pulse characteristics of the non-collaborative pulse. The detection performance and interference performance of the detection-jamming sharing signal based on VFFA are verified by a MATLAB simulation, and the validity of VFFA to solve the timing conflict problems of the detection-jamming sharing signal is analyzed.

4.1 Background and parameter setting

The experimental simulation is carried out using MATLAB in this paper. The experimental parameters are in line with the characteristics of typical medium or high PRF jagged signals. Set the following: the modulation bandwidth of the baseband intra-pulse linear frequency modulation signal is

5 MHz, the central frequency of the local oscillator is 10 GHz, and the signal pulse width is 1 μs. The two moving platforms fly head-on within 21 km of each other at speeds of 250 m/s and 300 m/s, respectively. In the background of this simulation experiment, the target uses the typical multi-jagged medium pulse repetition frequency (MPRF) signal to detect ourselves, and we use the detection-jamming shared signal based on VFFA proposed in this paper to detect and jam the target.

4.2 Interference performance analysis

Experiment 1 Simulation experiment of interference characteristics of shared signal

To verify the deceptive jamming effect of the shared signal on the non-collaborative radar, this experiment uses the MATLAB simulation platform to establish the non-collaborative radar visual angle and analyzes the jamming performance of the shared signal through the jamming situation of the non-collaborative radar. Taking two groups of coherent processing interval (CPI) as an example, the PRFs are 25 kHz and 33.3 kHz, and the number of CPI pulses in each group is 64.

Figure 5.(a) is the time-frequency analysis diagram of the non-collaborative radar after signal processing for the group with PRF_1 = 25 kHz under different signal-to-noise ratio (SNR) circumstances. The non-collaborative radar screen appears to the information of multiple false targets after receiving the target echo signal and the detection-jamming shared signal. As shown in Fig. 5.(b), that is the group diagram with PRF_2 = 33.3 kHz. By using the multi-PRF ambiguity-resolution method of remainder theorem, the multi-jagged signal can get the corresponding target distance values and velocity values, as shown in Table 1.

As the detection-jamming shared signal and the non-collaborative detection of echo signal enter the non-collaborative radar receiver, the power value will decrease as the SNR decreases. Although the non-collaborative uses multi-PRF ambiguity-resolution method, it still cannot distinguish the false target signal from the real echo signal, which causes a kind of deceptive interference with high accuracy to the non-collaborative.

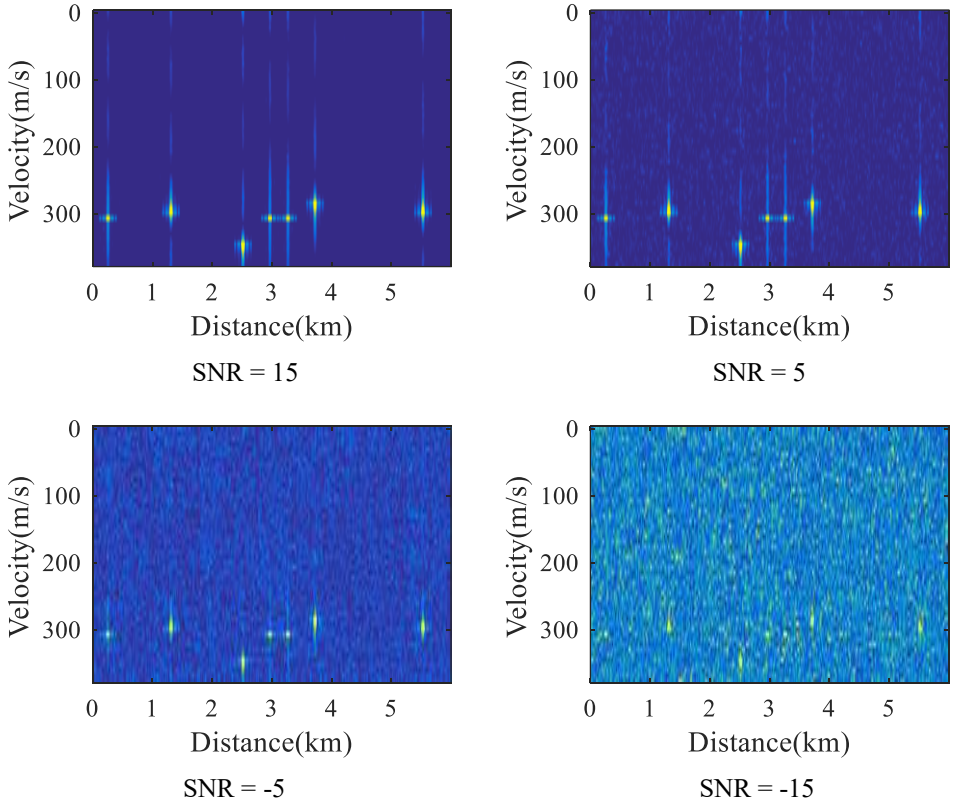

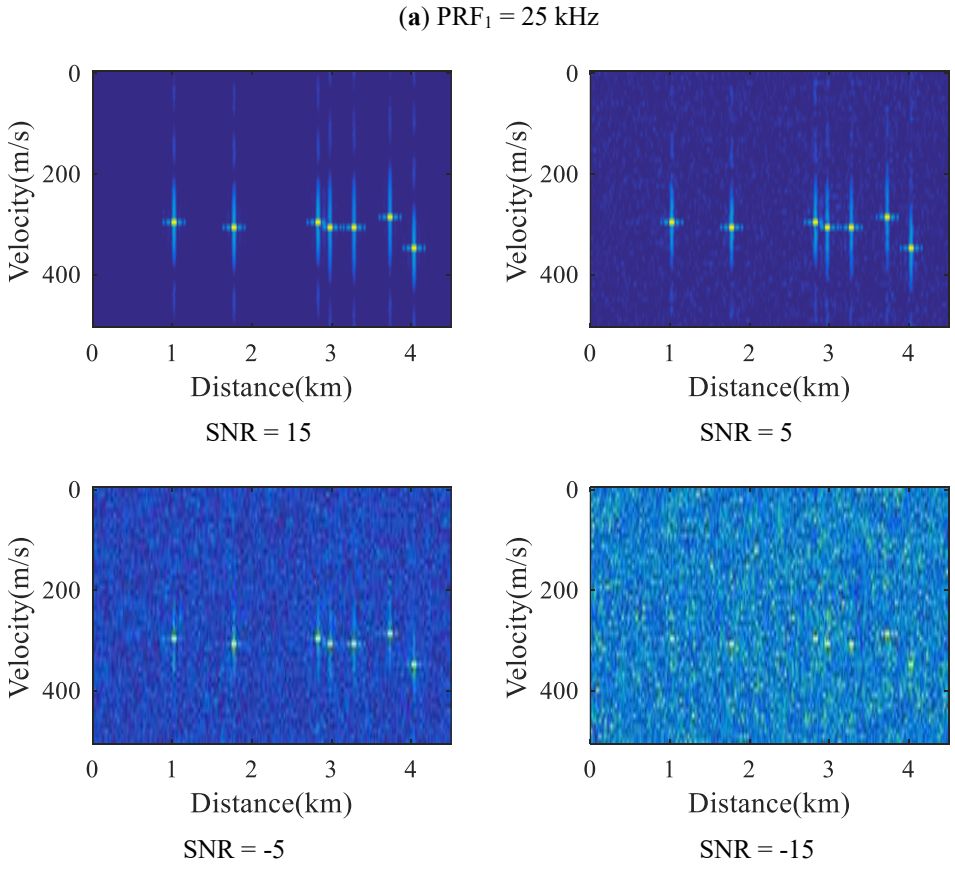

Fig. 5. The time-frequency analysis diagram of the non-collaborative radar.

Table 1 Results of multi-frequency ambiguity-resolution

Parameter Information	Distance (km)	Velocity (m/s)
Target 1	15.3	305
Target 2	21.0	305
Target 3	21.3	305
Target 4	21.75	285
Target 5	23.55	300
Target 6	25.35	300
Target 7	26.55	345

4.3 Detection performance analysis of shared signal

Because the detection-jamming shared signal takes the non-collaborative pulse signal as the sample, it is not enough to analyze the advantage of the shared signal's detection performance from the perspective of a fuzzy function. Therefore, through the MATLAB simulation platform, this section establishes an integrated detection-jamming system. After signal sorting, recognition, signal reconstruction, and pulse accumulation of echo signals of detection-jamming shared signals, the distance and velocity measurement error angles of the non-collaborative targets are finally analyzed and discussed. The detection superiority and signal processing superiority of our detection-jamming shared signal are analyzed and demonstrated.

Experiment 2 Velocity measurement and ranging performance simulation experiment

To verify the advantages of the detection-jamming shared signal over the maximum non-ambiguity ranging and velocity measurement, this experiment was carried out following the signal processing of the shared signal's echo signal; it involved signal reconstruction, distance and velocity measurements, and time-frequency analysis. By contrasting the ability of the non-ambiguity distance measurement and velocity measurement between the detection-jamming shared signal and the target transmitted signal, the advantage of detection-jamming shared signal was determined.

Because the target uses a multi-jagged MPRF signal, the maximum non-ambiguity range of the target is 18 km, and the maximum non-ambiguity velocity measurement is 500 m/s, we adopt the detection-jamming shared signal based on VFFA, which is optimized with the attributes of multi-PRF detection and multi-false-target jamming. Therefore, it effectively measures that the maximum non-ambiguity ranging of detection-jamming shared signal is equal to 126 km, the maximum non-ambiguity velocity measurement is much larger than the target's. As shown in Fig. 6, there is no ambiguity for velocity measurement, but there is a great advantage in ranging. Figure 7 displays a group of comparison graphs in which the detection range of range and velocity information is adjusted to the target area under different SNR conditions. After parameter measurement, it can be found that there is a moving target with a relative velocity of about 550 m/s within the space range of 21 km. Therefore, after VFFA, the multi-PRF detection-jamming shared signal with the optimal multi-dimensional characteristic parameters of the multiple false targets is obtained, which has a higher maximum non-ambiguity range and maximum non-ambiguity velocity measurement than the non-collaborative detection signal and can implement unambiguous detection for targets with longer distance and higher velocity.

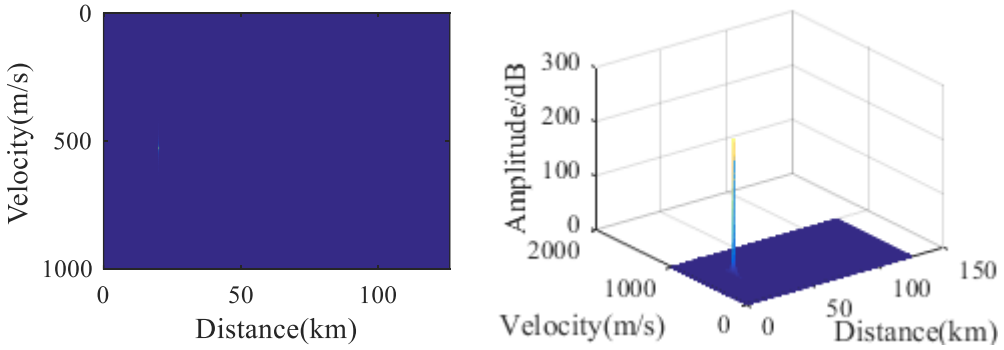

(a) The planar graph of time-frequency analysis (b) The three-dimensional graph of time-frequency

Fig. 6 The time-frequency overview of the integrated system

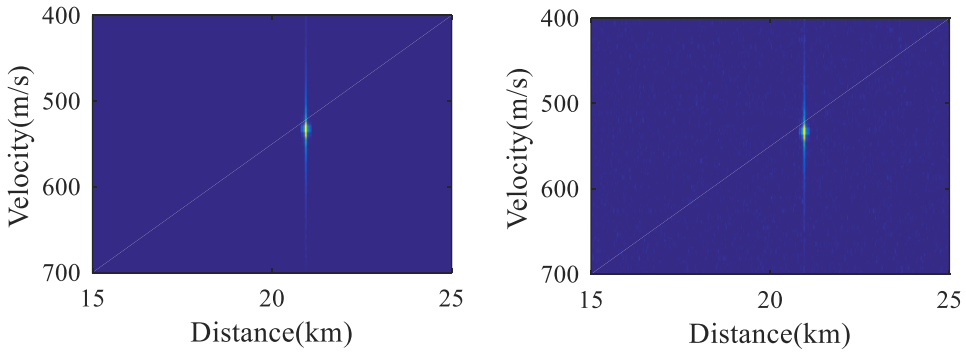

SNR = 15 SNR = 5

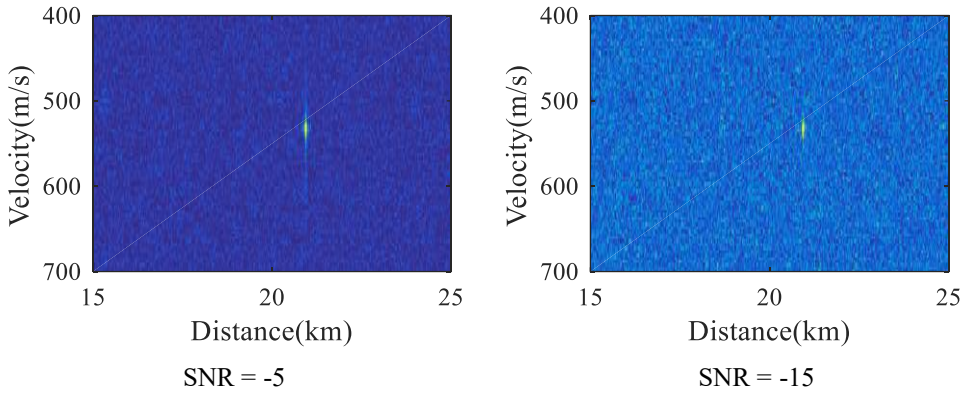

Fig. 7. Local time-frequency map of the integrated system.

Experiment 3 Simulation experiment of distance measurement and velocity error

In order to further verify the signal processing advantage of the detection-jamming shared signal, based on experiment 2, the influences of the pulse accumulation number on the range measurement error and the velocity measurement error are discussed and analyzed by taking the number of pulses as the independent variable and the ranging error and velocity measurement error as the dependent variables.

As shown in Fig. 8, due to the linear frequency modulation signal adopted in the pulse, the distance measurement error is almost zero. The error of velocity measurement decreases gradually with the increase of the number of accumulated pulses. When the target receives and accumulates an echo pulse, we can receive and accumulate more echo signal pulses at the same time within a PRI. As the pulse accumulation number increases, the multiple of echo signal SNR is raised and velocity measurement error is decreased obviously (velocity measurement error can be reduced to 5 m/s). This is the advantages of signal processing for pulse accumulation.

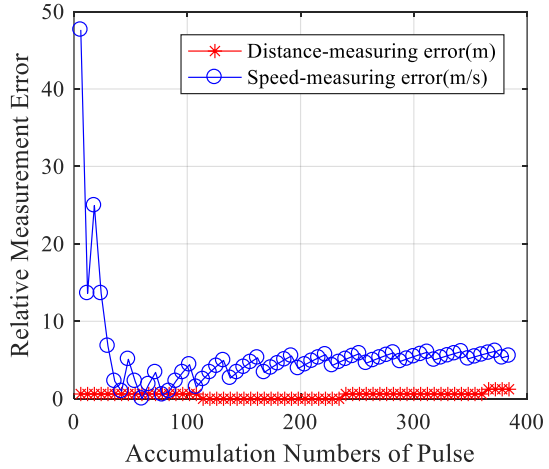

Fig. 8. The analysis of measurement error.

4.4 Effectiveness analysis of VFFA

Experiment 4 Simulation experiment of the algorithm effectiveness analysis

The purpose of this experiment was to explore whether the detection-jamming shared signal based on VFFA can solve the problems of timing conflict and pulse overlapping sequence. First, the integrated detection-jamming system was set up in MATLAB. Then, the system was analyzed to

determine whether the reconnaissance channel, interference channel, and detecting channels exhibited temporal isolation. As shown in Fig. 9, the integrated detection-jamming system after the adaptive processing of the VFFA will automatically switch the channels of reconnaissance, jamming, and detection, and the signals in the three channels will not interfere with or affect each other in the timing sequence.

As shown in Fig. 9(b), after the PRF of the non-collaborative signal is changed, no signal is received after the reconnaissance channel is opened, and there are signal overlaps and timing conflicts between the jamming channel and the detection channel. In this case, when we had a silent cycle of the integrated detection-jamming system and received the target transmitted signal, we would regard the target transmitted signal as our emission sample of the detection-jamming shared signals and optimizes in again false target multidimensional characteristics of detection-jamming shared signal by using VFFA. As shown in Fig. 9(c), after receiving the non-collaborative detection sample signal and being optimized by the algorithm, the new detection-jamming shared signal can be sent to detect and jam the target continuously. Because the algorithm retains as much of the original false target information as possible, the non-collaborative cannot filter our false target through the information of the temporal diagram or distance correlation, which greatly enhances the deceptive effect of the detection-jamming shared signal.

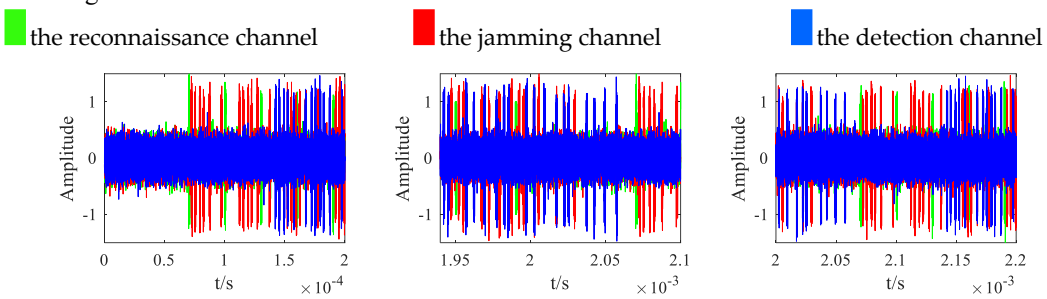

(a) The first period **(b)** The observation period **(c)** The next period when PRF is changed

Fig. 9. Schematic diagram of typical working process of integrated detection-jamming system.

The above analysis of the experimental data shows that the detection-jamming shared signal based on VFFA with optimized false target multi-dimensional characteristics not only has highly realistic target deceptive jamming but also presents a better detecting effect than the target. Further, it can be implemented at a higher gain of target distance and velocity measurement through signal processing in an integrated detection-jamming system for the echo signal, such as signal sorting and identification, signal reconstruction, and pulse accumulation. Because this article uses the linear frequency modulation signal in intra-pulse modulation, the detection-jamming shared signals reflect several advantages, among which the main advantage is that the ranging error is close to zero. With the continuous accumulation of pulse, the final velocity measurement error is kept at about 5 m/s. In addition, the integrated detection-jamming system effectively solves the time sequence conflict and pulse overlap of the three channels of reconnaissance, jamming, and detection, providing strong support for the future realization of integrated detection-jamming systems.

Conclusions and Future Work

In this paper, by making full use of VFFA's advantages, such as simple operation, fast convergence speed and real-time obstacle avoidance, a multi-objective and multi-dimensional characteristic parameter optimization model based on VFFA is established to design a detection-jamming shared signal waveform. The detection-jamming shared signal based on VFFA exhibits satisfactory deceptive jamming because the non-collaborative radar cannot distinguish the

false target signal from the real echo signal. The false target multi-dimensional characteristic parameters based on VFFA have high stability, making it impossible for the non-collaborative radar to determine whether the targets are real or false. In addition, the shared signal has a stronger ability of non-ambiguity ranging and non-ambiguity velocity measurement as well as better signal processing. In the same signal processing cycle, the detection-jamming shared signal based on VFFA can realize real-time detection of non-collaborative targets with better detection performance to effectively solve the problems of time-sequence conflict and pulse overlap among the reconnaissance, jamming, and detection channels. The detection-jamming shared signal based on VFFA is thus a highly feasible plan for optimizing the design of shared signal waveform. The detection-jamming shared signal based on VFFA also provides a new idea for future integrated electronic systems.

The implementation of the detection-jamming shared signal based on VFFA, however, has higher requirements for the credibility of the radar database data information. Therefore, the detection-jamming shared signal based on VFFA has a low data fault-tolerance rate. When the radar database data error is bigger, it will influence the optimal results of the false target parameters based on VFFA, further influencing the detection performance and interference effects of the detection-jamming shared signal. Therefore, future research must improve the fault tolerance rate of the algorithm and enhance the adaptability of the shared signal.

Acknowledgements

A short paragraph specifying their individual contributions should be declared with several authors for the research articles: Conceptualization, G.X.(Guomiao Xiong), Y.L.(Yunpeng Li) and C.C.(Chao Chen); Methodology, G.X.; Software, G.X. and C.C.; Validation, G.X., Y.L. and C.C.; Formal Analysis, G.X., Y.L. and C.C.; Investigation, Y.L. and C.C.; Resources, Y.L. and C.C.; Data Curation, G.X.; Writing – Original Draft Preparation, G.X.; Writing – Review & Editing, G.X., Y.L. and C.C.; Supervision, Y.L. and C.C.; Project Administration, C.C.; Funding Acquisition, Y.L.

Conflict of interest

Authors have no conflict of interest relevant to this article.

Reference

[1] XU Cuichun, CHEN T Q. Conception of “Signal Sharing” in Integrated Radar and Jammer System and the Integrated Signal Design[J]. College of Electronic Engineering, 2002,502-505.

[2] XU Cuichun. Conception of “Signal Sharing” in Integrated Radar and Jammer System and the Integrated Signal Design[D]. Chengdu: University of Electronic Science and Technology of China,2002.

[3] ZHANG Yong. Chaotic Integrated System of Radar and Jammer and Its Sharable Signal[D]. Chengdu: University of Electronic Science and Technology of China, 2006.

[4] ZHANG Yong. Integrated System of Radar and Jammer and Its Sharable Signal[M]. Xian: Xidian University Press, 2011.6.

[5] ZHONG Pan. Research on integrated signal of radar detection and jamming[D]. Chengdu:

University of Electronic Science and Technology of China, 2007.

[6] SHAO Chunping, TANG Shuangtian. Optimization Research of Radar and Jammer Integration Share Signal Design[J]. Microcomputer Information, 2010, 26 (28): 208-210+238.

[7] YANG Dandan, LIU Yian, TANG Shuangtian, et al. Optimization Design of Radar/Jammer Share Signal Modulated by Binary Phase Encoding Signal of Chaos[J]. Computer Integrated Manufacturing Systems, 2011, 28(06):30-33+37.

[8] TIAN L Y, HE M, LIU B, et al. Novel non-coherent integration method using binary phase-coded radar signal[J]. Journal of Beijing Institute of Technology 2013, 22(1):60-66.

[9] WEN Shuai. Study on Random Frequency-Hopping Signal Shared by Detection and Jamming[D]. Yangzhou: China Ship Research and Development Academy, 2018.

[10] TAN Long, JIANG Qiuxi, LIU Fangzheng. Detection and Jamming Integration Signal of Orthogonal Comb Waveform[J]. Journal of Detection and Control, 2016, 38(02):78-81+87.

[11] LI Qihu, WANG Ying, SHANG Kaishuan. Design and Performance Simulation for the Detection and Jamming Integrated Signal Waveform[J]. Journal of Detection and Control, 2020, 42(01):39-43.

[12] TANG Xiaodong. The Integrated Jammer and Radar System and Their Signal Sharing[J]. Modern Radar, 2012, 34(07):5-7+11.

[13] YANG Dandan, LIU Yian, TANG Shuangtian, et al. Design method of noise-phase-coded modulation integration signal[J]. Computer Engineering and Design, 2011, 32(01):354-357.

[14] CHEN Y J, BAI G W, ZHANG J M. Improvement of the Virtual Potential Field Based on Coverage-enhancing Algorithm for Directional Sensor Networks[J]. Journal of Chinese Computer Systems, 2013,34 (2): 243-246.

[15] DAI N. A Virtual Potential Field Based Coverage-Enhancing Algorithm for Directional Sensor Networks[D]. Kunming： Kunming University of Science and Technology, 2014.

[16] TAO D, MA H D, LIU L. A Virtual Potential Field Based Coverage-Enhancing Algorithm for Directional Sensor Networks[J]. Journal of Software, 2007,18 (5): 1152-1163.

[17] DAI N, MAO J L, FU L X, et al. Virtual potential field based coverage optimization algorithm for directional sensor networks[J]. Application Research of Computers, 2007,18 (5): 1152-1163.

[18] TAO D. Research on Coverage Control and Cooperative Processing Method for Video Sensor Networks[D]. Beijing: Beijing University of Posts and Telecommunications, 2007,18 (5): 1152-1163.

[19] JIANG Yibo, CHEN Qiong, WANG Wanliang, et al. A K level Coverage Enhancement Algorithm Based on Moving Target Trajectory Prediction for Video Sensor Networks[J]. CHINESE JOURNAL OF SENSORS AND ACTUATORS, 2014, 27 (7): 956-963.

[20] TAO D, MA H D, LIU L. Study on Path Coverage Enhancement Algorithm for Video Sensor Networks[J]. ACTA ELECTRONICA SINICA, 2008,36 (7): 1291-1296.

[21] YU W Q. Research on Target Tracking and Conflict Warning Strategy and Algorithm Based on Multi-sensor Fusion[D]. Shandong: Shandong University of Technology, 2020.

[22] ZHAO J, FU L. Integration design of radar and electronic warfare[J]. RADAR and ECM, 2015, 35 (3): 1-4.

[23] YU C L, ZHOU H F, YANG L, et al. Integrated System Design Technology of Tracking Radar and EW Equipment[J]. SHIPBOARD ELECTRONIC COUNTERMEASURE, 2014, 37 (4): 5-9.

[24] WANG M J. Integrated Technology of Reconnaissance and Jamming Based on Digital Channelization[J]. SHIPBOARD ELECTRONIC COUNTERMEASURE, 2018, 41 (3): 1-5.

[25] LIU C Y. Integration of Shipborne Fire Control Radar,Radar Reconnaissance and Active Jamming Equipment[J]. ELECTRONIC INFORMATION WARFARE TECHNOLOGY, 2012, 27 (5): 34-37.

[26] SUN B P. Design and Implementation of Integrative Equipment for Reconnaissance and Jamming with Wideband and High Sensitivity[D]. Chengdu: University of Electronic Science and Technology of China, 2019.

[27] ZHOU F Y, CHEN Z Y, ZHANG X R. Design of transceiver front-end for integration of radar or reconnaissance or jamming[J]. Journal of Air Force Early Warning Academy, 2014, 28 (6): 395-398.

[28] HE J H. FPGA Software Design for Reconnaissance and Jamming Integration Processor[D]. Harbin: Harbin Engineering University, 2017.

[29] GUAN Z F. Integrated Design of Multifunction RF System based on Software Defined Radio[J]. Communications Technology, 2014, 47 (11): 1333-1337.

[30] ZHAO P C. Structure and Development of Shipborne Radar /Electronic Warfare System[J]. Modern Radar, 2016, 38 (11): 15-17+60.

[31] WANG Z L, LIU J. Reconnaissance and jamming integration processing technique against coherent radar[J]. AEROSPACE ELECTRNIC WARFARE, 2009, 25 (2): 29-31.

[32] WU W B, NI J J, CHEN J F, et al. Approach of Robot Path Planning Based on Improved VFF[J].

MICROPROCESSORS, 2014, 3:48-51.

[33] WEI Z Y. Research on Intelligent Ship Track Control Based on Fuzzy Control[D]. Harbin: Harbin Engineering University, 2014, 3:48-51.

[34] HUANG Y Y. Research on Obstacle Avoidance of Indoor UAV Navigation Based on Data Fusion[D]. Chengdu: Chengdu University of Technology, 2017.

[35] YIN Z F, GAN S J, WU Z W, et al. Design and implementation of miniaturized UWB radio frequency conversion system[J]. AEROSPACE ELECTRNIC WARFARE, 2019,35 (1): 27-30.

[36] CHEN C B, ZHANG Y, GAO S. Method of Path Planning Based on Virtual Force Field and A* Algorithm[J]. Computer Systems and Applications, 2014,23 (9): 107-111.

[37] WANG W. Research on Sub-regional Dynamic Optimization Algorithm for Path Coverage in Wireless Video Sensor Networks[D]. Zhejiang: Zhejiang University of Technology, 2020.